Superconducting Ferromagnets

Introduction

In ferromagnets below the Curie temperature, T_C, the electron spins align to produce a net magnetization. For a long time it was thought that superconductivity is incompatible with ferromagnetism. This is rooted in the microscopic theory of superconductivity published in 1957 by Bardeen, Cooper, and Schrieffer (BCS). Within the standard BCS scenario, a superconducting condensate is formed under the influence of an attractive force due to lattice vibrations which binds electrons with antiparallel spins in singlet Cooper pairs. When magnetic impurity atoms are placed in a conventional superconductor, the local field surrounding the impurity atom suppresses singlet Cooper pair formation, which causes a rapid depression of the superconducting transition temperature, T_{sc}. Likewise, in superconductors which undergo a ferromagnetic transition below T_{sc} (because $T_C < T_{sc}$ these may be called ferromagnetic superconductors), the onset of long-range magnetic order is accompanied by the expulsion of superconductivity. Well-known examples of the competition of superconducting and magnetic ground states are found among the so-called Chevrel phases and borocarbides. However, around 1980, it was recognized that under special conditions superconductivity may coexist with antiferromagnetic order, where neighboring electron spins arrange in an antiparallel configuration. For instance, in heavy fermion antiferromagnets, the itinerant magnetic moments have almost no de-pairing effect on singlet Cooper pairs, because the average exchange interaction is zero.

The discovery of the first superconducting ferromagnet ($T_{sc} < T_C$) UGe_2 in the year 2000 came as a big surprise. In this material, superconductivity is realized well below the Curie temperature, without expelling the ferromagnetic order. Since then, three other superconducting ferromagnets have been discovered: UIr, URhGe, and UCoGe. These materials have in common that ferromagnetic order is due to the uranium $5f$ magnetic moments and has a strong itinerant character. Moreover, superconductivity occurs close to a magnetic instability. The coexistence of superconductivity and ferromagnetism in these materials can be understood in terms of spin fluctuation models: in the vicinity of a ferromagnetic quantum critical point, critical magnetic fluctuations can mediate superconductivity by pairing the electrons in spin-triplet Cooper pairs, that is, the equal-spin pairing (ESP) states $|\uparrow\uparrow\rangle$ ($L=1$, $S_z=1$) and $|\downarrow\downarrow\rangle$, ($L=1$, $S_z=-1$), and the state $(|\uparrow\downarrow\rangle + |\downarrow\uparrow\rangle)/\sqrt{2}$ with orbital momentum $L=1$ and projection of the spin momentum $S_z=0$. In this article, we present the superconducting ferromagnets known to date. We focus on materials where ferromagnetism and superconductivity are carried by the same electrons. This dismisses materials such as the cuprate $RuSr_2GdCu_2O_8$ and the borocarbide $ErNi_2B_2C$, where both phenomena are carried by different subsets of electrons. Notice that some form of coexistence of weak itinerant ferromagnetism and superconductivity has also been reported for the d-band metal Y_9Co_7. However, in this case, metallurgical problems have thwarted unraveling of the intrinsic properties.

1. Materials

The superconducting ferromagnets are listed in Table 1 together with several characteristic parameters. The crystal structure has a low symmetry, orthorhombic or monoclinic, which results in a strong uniaxial anisotropy of the electronic and magnetic properties. UGe_2 and UIr order ferromagnetically at the relatively high Curie temperature of 53 K and 46 K, respectively. Upon the application of mechanical pressure the magnetic state is depressed and superconductivity appears below 1 K for pressures exceeding 1.0 GPa. For URhGe and UCoGe ferromagnetism is weaker, with Curie temperatures of 9.5 K and 3 K, respectively, and superconductivity is found below 1 K at atmospheric pressure. The itinerant character of the ferromagnetic state is demonstrated by the small ratio of the ordered

Table 1
Ferromagnetic superconductors and characteristic parameters.

Material	Structure	T_C (K)	T_{sc} (K)	m_0 (μ_B/U atom)	p_{eff} (μ_B/U atom)	γ (J mol^{-1} K^{-2})
UGe_2	Orthorhombic	53	0.8[a]	1.5||a	2.9	0.032
URhGe	Orthorhombic	9.5	0.25	0.42||c	1.8	0.160
UIr	Monoclinic	46	0.1[b]	0.50||[10-1]	2.4	0.049
UCoGe	Orthorhombic	3	0.6	0.07||c	1.7	0.057

T_C, Curie temperature; T_{sc}, superconducting transition temperature; m_0, ordered moment; p_{eff}, Curie–Weiss effective moment; γ, linear coefficient in the specific heat.
[a]At a pressure of 1.2 GPa.
[b]At a pressure of 2.7 GPa.

moment m_0 over the high-temperature Curie–Weiss moment p_{eff}. The enhanced coefficient γ of the linear term in the electronic specific heat shows that these materials are correlated metals, but the electron–electron interactions are relatively weak.

1.1 UGe$_2$

This metal adopts an orthorhombic crystal structure (space group C_{mmm}). It orders ferromagnetically at $T_C = 53$ K with a fairly large ordered moment m_0 of $1.5\,\mu_B$ per U atom directed along the crystallographic *a*-axis. The pressure–temperature phase diagram is shown in Fig. 1. Ferromagnetic order is gradually depressed and vanishes by a first-order transition at a critical pressure $p_c = 1.6$ GPa. Superconductivity appears in the pressure range from 1 GPa up to p_c with a maximum $T_{sc} = 0.8$ K near 1.2 GPa. In the ferromagnetic phase an additional first-order phase transition takes place at $T_x(p)$ between a high-temperature low-moment ($\sim 1\,\mu_B$) phase FM1 and a low-temperature high-moment ($\sim 1.5\,\mu_B$) phase FM2. The phase line ends where $T_{sc}(p)$ has its maximal value. This has been taken as evidence that critical magnetic fluctuations associated with the first-order transition between the FM1 and FM2 states with different polarizations are responsible for superconductivity. This idea has been supported by a Stoner model in which spin-triplet superconductivity in the ferromagnetic phase is driven by tuning the majority spin Fermi level through a peak in the paramagnetic density of states, related to the change in polarization. In this model, superconductivity is driven by a change in the Fermi surface topology.

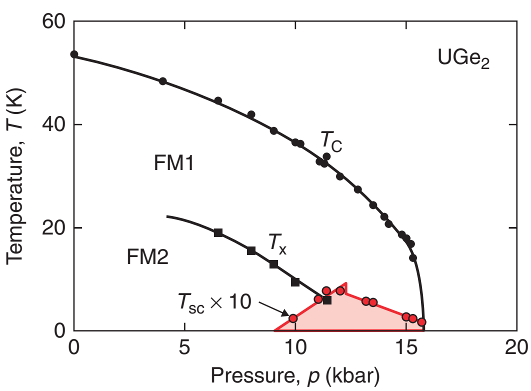

Figure 1
Phase diagram of UGe$_2$ determined by magnetization measurements under pressure. T_C is the Curie temperature and T_x locates the phase transition between two ferromagnetic phases FM1 and FM2 with different polarization. The pressure variation of the superconducting transition temperature T_{sc} ($\times 10$) is determined by electrical resistivity measurements. Reprinted with permission from Pfleiderer C, Huxley A D 2002 Pressure dependence of the magnetization in the ferromagnetic superconductor UGe$_2$. *Phys. Rev. Lett.* **89** (147005), 1–4, copyright (2002) by the American Physical Society.

1.2 UIr

This compound crystallizes in a monoclinic structure (space goup $P2_1$). The Curie temperature is 46 K and the ordered moment $m_0 = 0.5\,\mu_B$ per U atom points along the [1 0 –1] direction in the (010) plane. The pressure–temperature phase diagram is reproduced in Fig. 2. It consists of three magnetic phases (FM1, FM2, and FM3) and a superconducting phase. Under hydrostatic pressure $T_{C1} = 46$ K of the FM1 phase is depressed and vanishes at a critical pressure $p_{c1} \sim 1.7$ GPa. The FM2 phase with a reduced ordered moment of $0.08\,\mu_B$ appears near 1.2 GPa and vanishes at $p_{c2} \sim 2.1$ GPa. The FM3 phase with $m_0 = 0.07\,\mu_B$ phase appears above 1.4 GPa and smoothly disappears near $p_{c3} \sim 2.8$ GPa. This indicates that the ferro-to-paramagnetic transition near p_{c3} as a function of pressure is a second-order phase transition. The magnetic phase diagram is not fully understood yet. Experiments indicate that in the intermediate pressure range (1.5–2.2 GPa) an anomalous electronic state is

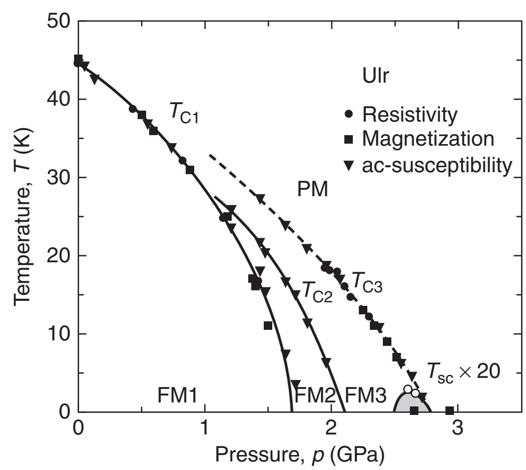

Figure 2
Phase diagram of UIr determined by resistivity, magnetization, and ac-susceptibility measurements under pressure. Three ferromagnetic phases FM1–3 are found. Superconductivity at T_{sc} ($\times 20$) occurs in the FM3 phase near the ferromagnetic quantum critical point. Adapted from Kobayashi T C, Fukushima S, Hidaka H, Kotegawa H, Akazawa T, Yamamoto E, Haga Y, Settai R, Onuki Y 2006 Pressure-induced superconductivity in ferromagnet UIr without inversion symmetry. *Physica B* **378–80**, 355–8.

induced, possibly due to a multilayer-like magnetic phase separation. Superconductivity is found in a small pressure range between 2.6 GPa and p_{c3} in the FM3 phase, with a maximum $T_{sc} = 0.14$ K. An interesting aspect is that the crystal structure of UIr is noncentrosymmetric, which was first thought to prevent the formation of spin-triplet Cooper pairs. While ferromagnetic order breaks time-reversal symmetry and lifts the spin degeneracy, thus favoring spin-triplet superconductivity, the lack of inversion symmetry lifts the degeneracy between **k** and –**k** states, which in turn inhibits spin-triplet pairing. However, it has been recognized that in the case of strong spin–orbit interaction different spin states mix, and therefore one cannot distinguish between pure spin-triplet and -singlet states. Another possibility is that an inhomogeneous Fulde–Ferrel–Larkin–Ovchinnikov phase is realized, where electrons with **k** and $-\mathbf{k}+q$ can form Cooper pairs with nonzero momentum. The location of the superconducting pocket in the FM3 phase close to the border of ferromagnetism indicates that superconductivity is driven by critical magnetic fluctuations associated with a ferromagnetic quantum critical point.

1.3 URhGe

This material belongs to the large family of uranium 1:1:1 intermetallics. The crystal structure is orthorhombic (space group P_{nma}). Ferromagnetic order is observed below $T_C = 9.5$ K and the uniaxial spontaneous moment of $0.42\,\mu_B$ per U atom is directed along the *c*-axis. Spin-triplet superconductivity is observed at atmospheric pressure deep in the ferromagnetic phase below $T_{sc} = 0.25$ K. Under hydrostatic pressure, ferromagnetic order is not suppressed, as shown in Fig. 3, but T_C increases at a rate of $0.65\,\text{K}\,\text{GPa}^{-1}$ up to the highest pressures measured (13 GPa). This phase diagram is distinctly different when compared to the *p*–*T* diagrams of UGe_2, UIr, and UCoGe, which obey the more commonly observed Doniach-like behavior for magnetic order in correlated metals: the magnetic transition temperature is reduced when the product $JN(E_F)$ increases under the influence of mechanical pressure (here J is the exchange interaction and $N(E_F)$ the density of states at the Fermi level). On the other hand, the hybridization phenomena leading to magnetic order are most likely strongly anisotropic, and it cannot be excluded that under uniaxial rather than hydrostatic pressure a Doniach-like phase diagram results. While T_C steadily increases under hydrostatic pressure, superconductivity is depressed and vanishes near 3.0 GPa. Solid evidence for triplet superconductivity has been extracted from measurements of the upper critical field B_{c2}. At 0 K, B_{c2} exceeds the paramagnetic Pauli limit and the temperature variation $B_{c2}(T)$ is well described by the model function for a superconducting gap with a line node (polar gap) and the maximum gap parallel to the *a*-axis. Surprisingly, a highly interesting phenomenon occurs for strong magnetic fields directed along the orthorhombic *b*-axis. Superconductivity is first suppressed at $B_{c2} \sim 2$ T, but reappears when the applied field exceeds 12 T. The field-induced superconducting phase is connected to a spin re-orientation process: when the component of the field along the *b*-axis reaches 12 T, the ordered moment rotates from the *c*-axis towards the *b*-axis. Compelling evidence has been provided that the high-field, as well as the low-field, superconducting state is mediated by critical magnetic fluctuations associated with the field-induced spin-reorientation process. Near the quantum critical point, an acute enhancement of the critical field for the suppression of superconductivity has been observed, and superconductivity, although it never occurs above 0.5 K, can survive in extremely high fields as large as 28 T.

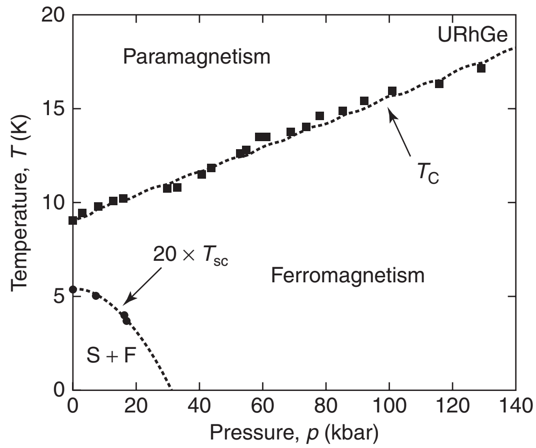

Figure 3
Phase diagram of URhGe. The Curie temperature as determined by ac-calorimetry. Ferromagnetism is present up to pressures of 13 GPa. The superconducting transition temperature T_{sc} ($\times 20$) is determined by electrical resistivity. From Hardy F, Huxley A D, Flouquet J, Salce B, Knebel G, Braithwaite D, Aoki D, Uhlarz M, Pfleiderer C 2005 (*P*, *T*) phase diagram of the ferromagnetic superconductor URhGe. *Physica B* **359–61**, 1111–13.

1.4 UCoGe

This uranium 1:1:1 compound forms in the same orthorhombic crystal structure (space group P_{nma}) as URhGe. Itinerant ferromagnetic order is weak, with a Curie temperature of 3 K and a small ordered moment of $0.07\,\mu_B$ per U atom. The ferromagnetic structure is uniaxial with $m_0 || c$. Superconductivity is observed at

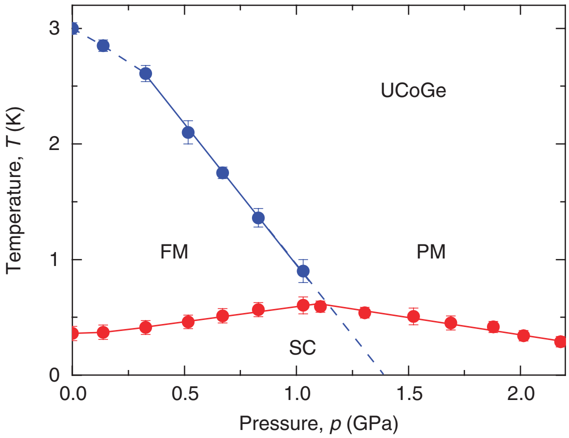

Figure 4
Phase diagram of UCoGe determined by ac-susceptibility under pressure. Ferromagnetism is not observed for $p > 1.1$ GPa. Notice the superconducting phase at high pressures does not break time-reversal symmetry.

atmospheric pressure in the ferromagnetic phase with $T_{sc} = 0.6$ K. The ratio $T_{sc}/T_C \approx 0.2$ is the largest among the superconducting ferromagnets. For UIr T_{sc}/T_C is 0.1 (at 2.7 GPa where T_{sc} is maximum), while for UGe_2 and URhGe the ratio is almost one order of magnitude smaller ($\sim$0.02–0.03). Measurements of the upper critical field B_{c2} support triplet superconductivity and point to an axial superconducting gap function with nodes along the *c*-axis, that is, the direction of the ordered moment m_0. The B_{c2} curves show an unusual upward curvature ($B \parallel b$) or kink ($B \parallel a$), which is possibly due to a competition between the equal-spin pairing states $|\uparrow\uparrow\rangle$ and $|\downarrow\downarrow\rangle$, expected for a two-band ferromagnetic superconductor. Under hydrostatic pressure, ferromagnetism is depressed, while the superconducting transition temperature first increases, as shown in Fig. 4. However, for $p > 1.0$ GPa, ferromagnetic order is no longer observed. This *p*–*T* phase diagram differs from the diagrams measured for the other superconducting ferromagnets, notably because superconductivity survives in the paramagnetic regime up to the highest pressures (2.2 GPa). In the ferromagnetic phase time-reversal symmetry is broken, and spin-orbit coupling restricts the Cooper states to the ESP states $|\uparrow\uparrow\rangle$ or $|\downarrow\downarrow\rangle$. The high-pressure ($p >$ 1.0 GPa) superconducting phase does not break time reversal symmetry and is possibly a planar spin-triplet or a conventional spin-singlet state.

2. *Theory Considerations*

A qualitative explanation for the occurrence of superconductivity in itinerant ferromagnets is offered by spin fluctuation models. In the simplest form, the magnetic behavior is described by a mean-field theory in terms of a Hubbard-type exchange interaction parameter $\bar{I}$ and a Stoner enhancement factor $S = (1 - \bar{I})^{-1}$. As $\bar{I}$ is tuned to the critical value $\bar{I} \rightarrow 1$, a second-order quantum phase transition takes place from the paramagnetic to the ferromagnetic state. Near the critical point, the exchange of longitudinal spin fluctuations can mediate *p*-wave superconductivity. In the ferromagnetic phase, exchange splitting of the Fermi surface results in the separation in majority and minority spin sheets. For a sizeable Fermi surface splitting superconductivity is necessarily restricted to the ESP states, $|\uparrow\uparrow\rangle$ and $|\downarrow\downarrow\rangle$, which form on the different Fermi surface sheets. Band-structure calculations for the superconducting ferromagnets confirm a large exchange splitting of the order of 10–100 meV. Thus, in principle, superconducting ferromagnets are two-band superconductors: upon lowering the temperature in the ferromagnetic phase, first the ESP state $|\uparrow\uparrow\rangle$ is formed, and by further lowering the temperature the ESP state $|\downarrow\downarrow\rangle$ is formed. Whether both superconducting phases are present depends sensitively on the details of the band structure. Hitherto, only in the case of UCoGe, a possible signature of two-band superconductivity has been reported. In the spin-fluctuation model, coexistence of superconductivity and ferromagnetism takes place on the microscopic scale, because the same electrons are responsible for band ferromagnetism and superconductivity. At the critical point superconductivity is suppressed, but is predicted to reappear in the paramagnetic phase ($\bar{I} < 1$), with a transition temperature comparable to the one in the ferromagnetic phase. In the paramagnetic phase, in the absence of a magnetic field, all three components of the triplet state are equivalent and have the same T_{sc}. In the case of UGe_2 and UIr, a superconducting phase for $p > p_c$ has not been detected (see Figs. 1 and 2). An explanation for this has been offered by an additional ingredient in the model: magnons (ferromagnetic spin waves) couple to the longitudinal magnetic susceptibility, which enhances T_{sc} to experimentally accessible values in the ferromagnetic phase ($p < p_c$) only.

The simple model portrayed above may serve as a starting point for understanding *p*-wave superconductivity in itinerant ferromagnets. Possibly it yields an adequate description for UIr where superconductivity occurs at the border of a second-order ferromagnetic phase transition. However, the *p*–*T* phase diagrams reproduced in Figs. 1, 3, and 4 imply that more sophisticated models are needed. For UGe_2, superconductivity seems to be driven by critical fluctuations associated with a field-induced first-order transition between two phases with different polarization. In URhGe, the critical point for ferromagnetism cannot be reached by the application of pressure, but superconductivity reappears near a field-induced quantum critical point. Finally, the p–T diagram of UCoGe shows ferromagnetism is gradually depressed and vanishes at a quantum critical point $p_c \approx 1.4$ GPa. However near p_c T_{sc} goes through a maximum rather than a minimum, in contradiction to the spin-fluctuation model sketched above.

The superconducting state in superconducting ferromagnets is unconventional because (i) Cooper pairing is magnetically mediated and (ii) the superconducting gap structure has a lower symmetry than the crystal lattice. Symmetry-group considerations have been very useful in discriminating the possible superconducting gap functions. In the paramagnetic state ($T > T_C > T_{sc}$) the symmetry group is given by $G^{sym} = G \times T \times U(1)$, where G represents the point-group symmetry of the lattice, T denotes time-reversal symmetry, and $U(1)$ is the gauge symmetry. In the ferromagnetic phase ($T < T_C$) time-reversal symmetry is broken, and in the superconducting phase ($T < T_{sc} < T_C$) gauge symmetry is broken as well. For uniaxial ferromagnets with an orthorhombic crystal symmetry, such as UGe_2, URhGe, and UCoGe, the allowed superconducting gap functions have been worked out in detail. The order parameter basis functions belong to different co-representations of the symmetry group of the initial ferromagnetic state and, in general, give rise to different critical temperatures. Taking into account spin–orbit coupling and under the assumption that the exchange splitting of the Fermi surface is sufficiently large, such that the pairing between electrons from spin-up and -down bands is negligible, ESP will give rise to two-band superconductivity with gap functions $\Delta_{\uparrow\uparrow}(R,k) = -\eta_1(R)f_-(k)$ and $\Delta_{\downarrow\downarrow}(R,k) = \eta_2(R)f_+(k)$, where $\eta_{1,2}$ are the order parameter amplitudes (R is a space coordinate and k is the momentum). From the symmetry-group analysis, it follows that only two superconducting gap structures $f_\pm(k)$ are possible. Assuming that the ordered moment m_0 is directed along the z-axis (as for a uniaxial ferromagnet), then the superconducting gap has zeros (nodes) parallel to the magnetic axis ($k_x = k_y = 0$, A phase) or a line of zeros in the k_x–k_y plane of the Fermi surface ($k_z = 0$, B phase). In other words, the A phase has a gap function of axial symmetry with nodes along m_0 and the B phase has a gap of polar symmetry with a line of nodes perpendicular to m_0. Using the results from the symmetry-group analysis, upper critical field data of URhGe and UCoGe provide evidence for a polar and axial state, respectively.

3. Concluding Remarks

Although superconductivity in ferromagnets was predicted more than 30 years ago, it took many years before the first material UGe_2 was discovered. This is most likely due to the extreme experimental conditions required. The material under investigation should be close to itinerant ferromagnetic order, which might necessitate the application of large pressures. Next, samples should be sufficiently clean, that is, the electronic mean free path l should be larger than the superconducting coherence length ξ, because impurities are detrimental to spin-triplet Cooper pairing. Another barrier is that the superconducting transition temperatures are very low, and cooling to the subkelvin temperature range is necessary. Finally, the presence of a strong magnetic anisotropy, which gives rise to a reduced dimensionality of the critical spin fluctuations, appears to be crucial. This possibly explains why superconductivity has not been found in clean d-band ferromagnetic metals.

Research in superconducting ferromagnets has just begun. The p–T and B–T phase diagrams have been established for UGe_2, UIr, URhGe, and UCoGe. However, precise measurements of the electronic and magnetic excitation spectra in the superconducting and magnetic phases, which are expected to reveal crucial information on the superconducting gap structure and pairing mechanism, are in most cases still lacking. URhGe and UCoGe offer the advantage that such measurements can be performed at ambient pressure. The coexistence of superconductivity and ferromagnetism offers an attractive playground for the investigation of new phenomena, like the elusive spontaneous vortex lattice, which is expected to form when the internal field due to the ferromagnetic order is larger than the lower critical field B_{c1}, the influence of spin-triplet superconductivity on the ferromagnetic domain size, control of tunneling currents by magnetization, and so on. The interplay of magnetism and superconductivity is a central issue in the understanding of superconductivity itself. Research into ferromagnetic superconductors will help us to unravel how magnetic fluctuations can stimulate superconductivity. This fundamental insight might turn out to be crucial in the design of new superconducting materials with high transition temperatures.

See also: High-T_c Superconductors: Electronic Structure; High-T_c Superconductors: Magnetic Properties of Doped Cuprates; High-T_c Superconductors: Magnetic Properties of the Undoped Parent Compounds; Non-Fermi Liquid Behavior: Quantum Phase Transitions; Superconducting Materials, Types of; Superconductors: Borocarbides; Superconductors: Non-s-wave Pairing.

Bibliography

Aoki D, Huxley A D, Ressouche E, Braithwaite D, Flouquet J, Brison J P, Lhotel E, Paulsen C 2001 Coexistence of superconductivity and ferromagnetism in URhGe. *Nature (London)* **413**, 613–16

Fay D, Appel J 1980 Coexistence of *p*-state superconductivity and itinerant ferromagnetism. *Phys. Rev. B* **22**, 3173–82

Hardy F, Huxley A D, Flouquet J, Salce B, Knebel G, Braithwaite D, Aoki D, Uhlarz M, Pfleiderer C 2005 (*P*, *T*) phase diagram of the ferromagnetic superconductor URhGe. *Physica B* **359–61**, 1111–13

Huy N T, De Nijs D E, Huang Y, De Visser A 2008 Unusual upper critical field of the ferromagnetic superconductor UCoGe. *Phys. Rev. Lett.* **100** (077002), 1–4

Huy N T, Gasparini A, De Nijs D E, Huang Y, Klaasse J C P, Gortenmulder T, De Visser A, Hamann A, Görlach T, Von Löhneysen H 2007 Superconductivity on the border of weak itinerant ferromagnetism in UCoGe. *Phys. Rev. Lett.* **99** (067006), 1–4

Kobayashi T C, Fukushima S, Hidaka H, Kotegawa H, Akazawa T, Yamamoto E, Haga Y, Settai R, Onuki Y 2006 Pressure-induced superconductivity in ferromagnet UIr without inversion symmetry. *Physica B* **378–80**, 355–8

Kobayashi T C, Hori A, Fukushima S, Hidaka H, Kotegawa H, Akazawa T, Takeda K, Ohishi Y, Yamamoto E 2007 Pressure–temperature phase diagram and superconductivity in UIr. *J. Phys. Soc. Jpn.* **76** (051007), 1–11

Lévy F, Sheikin I, Grenier B, Huxley A D 2005 Magnetic-field-induced superconductivity in the ferromagnet URhGe. *Science* **309**, 1343–6

Mineev V P, Champel T 2004 Theory of superconductivity in ferromagnetic superconductors with triplet pairing. *Phys. Rev. B* **69** (144521), 1–6

Mineev V P, Samokhin K V 1999 *Introduction to Unconventional Superconductivity*. Gordon and Breach, New York

Monthoux P, Pines D, Lonzarich G G 2007 Superconductivity without phonons. *Nature (London)* **450**, 1177–83

Pfleiderer C, Huxley A D 2002 Pressure dependence of the magnetization in the ferromagnetic superconductor UGe_2. *Phys. Rev. Lett.* **89** (147005), 1–4

Saxena S S, Ahilan K, Agarwal P, Grosche F M, Haselwimmer R K, Steiner M, Pugh E, Walker I R, Julian S R, Monthoux P, Lonzarich G G, Huxley A D, Sheikin I, Braithwaite D, Flouquet J 2000 Superconductivity on the border of itinerant-electron ferromagnetism in UGe_2. *Nature (London)* **406**, 587–92

A. de Visser

Encyclopedia of Materials: Science and Technology
ISBN: 978-0-0804-3152-9
pp. 1–6